Plaque-Associated Vasa Vasorum in Aged Apolipoprotein E-Deficient Mice Exhibit Proatherogenic Functional Features In Vivo

Plaque-Associated Vasa Vasorum in Aged Apolipoprotein E–Deficient Mice Exhibit Proatherogenic Functional Features In Vivo

Timo Rademakers,* Kim Douma,* Tilman M. Hackeng, Mark J. Post, Judith C. Sluimer, Mat J.A.P. Daemen, Erik A.L. Biessen, Sylvia Heeneman, Marc A.M.J. van Zandvoort

Objective—Neovascularization of human atherosclerotic plaques is implicated in plaque progression and destabilization, although its functional implications are yet unresolved. Here, we aimed to elucidate functional and morphological properties of plaque microvessels in mice in vivo.

Methods and Results—Atherosclerotic carotid arteries from aged (>40 weeks) apolipoprotein E–deficient mice were imaged in vivo using multiphoton laser scanning microscopy. Two distinct groups of vasa vasorum microvessels were observed at sites of atherosclerosis development (median diameters of 18.5 and 5.9 μm, respectively), whereas microvessels within the plaque could only rarely be found. In vivo imaging showed ongoing angiogenic activity and injection of fluorescein isothiocyanate-dextran confirmed active perfusion. Plaque vasa vasorum showed increased microvascular leakage, combined with a loss of endothelial glycocalyx. Mean blood flow velocity in plaque-associated vasa vasorum was reduced by ±50% compared with diameter-matched control capillaries, whereas mean blood flow was reduced 8-fold. Leukocyte adhesion and extravasation were increased 6-fold in vasa vasorum versus control capillaries.

Conclusion—Using a novel in vivo functional imaging strategy, we showed that plaque-associated vasa vasorum were angiogenically active and, albeit poorly, perfused. Moreover, plaque-associated vasa vasorum showed increased permeability, reduced blood flow, and increased leukocyte adhesion and extravasation (ie, characteristics that could contribute to plaque progression and destabilization). **(*Arterioscler Thromb Vasc Biol*. 2013;33:249-256.)**

Key Words: angiogenesis ■ atherosclerosis ■ in vivo imaging ■ microcirculation ■ multiphoton laser scanning microscopy

Human atherosclerotic plaques are characterized by local expansion of the vasa vasorum and development of intraplaque microvasculature. The extent of vascularization has been shown to correlate with progression stage, inflammatory content of the plaque, and plaque instability.[1,2] Ever since Köster suggested that advanced atherosclerotic lesions are associated with an increased density in vasa vasorum,[3] a growing number of studies have shown that both intraplaque microvasculature and vasa vasorum expansion enhance human atherosclerotic plaque progression.[1,4,5] Intraplaque microvessels are thought to be derived mainly from the vasa vasorum by angiogenic sprouting, followed by ingrowth into the lesion.[6–8] The angiogenic response itself is considered to arise from the gradual development of lesional hypoxia attributable to (1) increased physical distance to the lumen, exceeding the diffusion distance of oxygen, and (2) increased local metabolic activity of the plaque's inflammatory content.[1,9] Additionally, the endothelium of the newly formed microvessels is prone to continuous exposure to inflammatory mediators, which could lead to impaired functionality and increased permeability, caused by deteriorated interendothelial junctions and basement membrane detachment.[10] Dysfunctional microvessels would favor influx of circulating erythrocytes, leukocytes, and blood platelets into the plaque,[6,7,11] thereby promoting plaque expansion, destabilization, and thrombogenicity.

Despite the clinical relevance of plaque neovascularization, experimental animal studies on functionality of plaque microvessels have been hampered by their low incidence, or even lack thereof, in mouse models of atherosclerosis. Proangiogenic interventions in murine models have shown to increase plaque development and disease burden,[12–16] whereas antiangiogenic therapy decreases atherosclerosis development,[17–20] implicating a potent role for angiogenesis in experimental atherosclerosis models. However, the interventions also influenced the

Received on: July 13, 2012; final version accepted on: November 27, 2012.

From the Departments of Pathology (T.R., J.C.S, M.J.A.P.D., E.A.L.B., S.H.), Biomedical Engineering (K.D.), Radiology (K.D.), Biochemistry (T.M.H.), Physiology (M.J.P.), and Molecular Cell Biology (M.A.M.J.v.Z.), Cardiovascular Research Institute Maastricht, Maastricht University, Maastricht; Department of Pathology (M.J.A.P.D.), Academic Medical Center, Amsterdam, The Netherlands; and Institute for Molecular Cardiovascular Research (M.A.M.J.v.Z.), RWTA Aachen University, Pauwelsstrasse, Aachen, Germany.

*These authors contributed equally to this article.

The online-only Data Supplement is available with this article at http://atvb.ahajournals.org/lookup/suppl/doi:10.1161/ATVBAHA.112.300087/-/DC1.

Correspondence to Timo Rademakers, Maastricht University, P. Debyelaan 25, Maastricht, 6229HX, the Netherlands. E-mail t.rademakers@maastrichtuniversity.nl

inflammatory response, thereby affecting lesion development independent of plaque neovascularization. In general, animal studies have failed to show a direct causal relation between plaque vascularization, on the one hand, and plaque progression and destabilization, on the other.

Lack of adequate detection tools also hampered functional studies of plaque microvessels. Several methods like magnetic resonance imaging[21,22] or micro- and nano-computed tomography[23] have been applied to investigate plaque vascularization in murine models of atherosclerosis. These methods lack the spatial and temporal resolution to detect functional and structural properties of individual microvessels, or to distinguish between the artery and microvessels. Also, these techniques lack the ability to detect multiple imaging probes simultaneously. Multiphoton laser scanning microscopy (MPLSM) can overcome these shortcomings and has previously been used for in situ imaging of healthy and atherosclerotic arteries at subcellular resolution,[24,25] as well as for quantifying angiogenic activity in models of tumor vascularization and myocardial infarction.[26,27] In addition, MPLSM has been used to image large blood vessels in vivo, triggered on heart rate and respiration to reduce motion artifacts.[28,29] More recently, MPLSM was used to quantify blood flow and hematocrit in blood vessels,[30] substantiating MPLSM as a valuable tool for functional studies of the (micro)vasculature.

Here, we studied plaque microvessels to elucidate their structural and functional characteristics. Using MPLSM imaging in a novel in vivo imaging strategy, plaque microvessels could be visualized in aged apolipoprotein E–deficient ($ApoE^{-/-}$) mice. More importantly, angiogenic activity could be visualized and functional characteristics, including blood flow, adhesion and extravasation of leukocytes, and microvascular permeability, could be quantified and were found to differ significantly from control microvascular beds.

Methods

Animals

For ex vivo and in vivo experiments, aged $ApoE^{-/-}$ mice (40–50 weeks of age; n=51) with advanced atherosclerotic plaques were used. Young $ApoE^{-/-}$ mice (12–16 weeks of age; n=8), without or with only initial atherosclerotic plaques, and age-matched wild-type C57Bl/6 mice (n=20) served as controls. Mice were supplied by the institutional animal facility and were housed in conventional cages and received a normal chow diet. Experiments were approved by the local animal ethics committee and performed according to institutional guidelines.

Imaging

MPLSM imaging was performed on a Leica SP5 imaging platform (Leica Microsystems) that integrates multiphoton microscopy with fast resonant scanning, and uses a Compact Ultrafast Ti:Sapphire Laser (Chameleon, Coherent). Anti-CD31 antibody (BD Pharmingen) was used to detect vascular endothelium, and cyclic Asn–Gly–Arg was used to target CD13, a marker of angiogenic vascular endothelium. Biotinylated anti–Ephrin-B2 and anti–EphB4 (R&D Systems) antibodies were used to assess arterial or venous lineage of microvessels, respectively. Biotinylated antibodies were conjugated with streptavidin-quantum dot 525 (green) or streptavidin-quantum dot 585 (red) as indicated. To examine perfusion of microvessels and microvascular permeability, 70- and 150-kDa fluorescein isothiocyanate-labeled dextrans (Sigma) were used. For studying blood flow and leukocyte trafficking, leukocytes were labeled using Rhodamin 6G or Cell Tracker Red (CMTPX, Invitrogen).

Statistics

Data are presented as mean±SEM, unless stated otherwise. Statistics were performed using Graphpad Prism 5.0 or PASW Statistics 18. The nonparametric Mann-Whitney *U* test was applied to adhesion, extravasation, and blood flow velocity data. Microvascular permeability data were analyzed using curve fitting regression analysis. Fisher exact test was used for examining differences between groups for presence of plaque-associated microvasculature. Results were considered statistically different when $P<0.05$. Expanded methods are available in the online-only Data Supplement.

Results

Vasa Vasorum Were Visualized and Morphologically Characterized In Vivo

The vasa vasorum were studied in detail using in vivo and in situ MPLSM after labeling with anti-CD31, allowing characterization of microvessel morphology throughout the adventitia. Characteristics like microvessel diameter were similar in the adventitia of the carotid artery and abdominal aorta (Table 1). Based on the size and orientation, 2 types of plaque-specific microvessels could be discriminated. The larger vasa vasorum microvessels (median diameter, 18.5 μm) generally ran in parallel to the artery, whereas smaller microvessels (median diameter, 5.9 μm) mostly covered the artery radially. The adventitia surrounding the atherosclerotic plaque showed several microvessels (Figure 1A and 1B, Movies I and II in the online-only Data Supplement), which was confirmed by immunohistochemistry for CD31 and von Willebrand factor (Figure I in the online-only Data Supplement). Microvessels in peri-adventitial fat were excluded from analysis based on collagen imaging of the adventitia using second harmonic generation and imaging of autofluorescence of the peri-adventitial fat. Microvessels were mostly situated within 40 to 80 μm from the outer elastic lamina, but occasionally—at sites of large advanced plaques—microvessels would be situated within 15 to 20 μm from the outer elastic lamina. Vasa vasorum were

Table 1. Quantification of Microvessel Diameter From Plaque-Associated Microvessels in the Carotid Artery and Abdominal Aorta.

	Location	Median, μm	Range, μm	Total No. of Microvessels (Total No. Mice)
Carotid artery	Intraplaque	6.65	4.42–9.02	6 (20)
	Adventitial (large; >10 μm)	18.5	10.5–21.2	71 (39)
	Adventitial (small; <10 μm)	5.9	5.56–6.23	56 (39)
Abdominal aorta	Intraplaque	ND	ND	ND
	Adventitial (large; >10 μm)	22.7	16.6–43.8	8 (8)
	Adventitial (small; <10 μm)	6.0	2.1–16.5	5 (8)

ND indicates not determined.

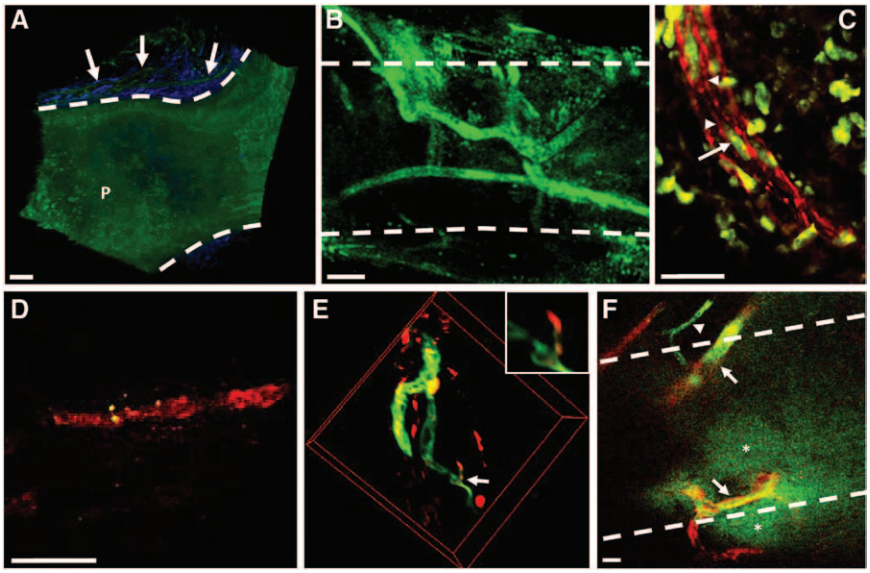

Figure 1. Plaque-associated vasa vasorum of atherosclerotic plaques at the carotid artery bifurcation in aged apolipoprotein E–deficient (ApoE$^{-/-}$) mice could be detected using multiphoton laser scanning microscopy (MPLSM). Three-dimensional rendering of the carotid artery directly proximal from the bifurcation and viewed from the luminal side depicts vasa vasorum (green, **arrows**) embedded in adventitial collagen (blue; **A**, Movie I in the online-only Data Supplement). Plaque autofluorescence in green (P) is also visible. When focusing merely on the adventitia, the vasa vasorum is clearly detectable (**B**, green; Movie II in the online-only Data Supplement). **C**, Single CD31^{+} (red, **arrowheads**) endothelial cells including nuclei (green, **arrow**) were detected. When assessing arterial/venous lineage of the vasa vasorum, microvessels were found to be predominantly arterial in origin as shown by Ephrin-B2 staining (**D**, red), whereas the venous marker Eph-B4 (green) was not detectable. Using a cyclic Asn–Gly–Arg (cNGR) probe (red, inset figure **E**) to detect angiogenic endothelium, angiogenic sprouting from a preexisting vasa vasorum vessel (green) was detected. CD31^{+} vasa vasorum vessels (red, **arrows**), as well as new sprouts (CD31^{low}, **arrowhead**), are actively perfused as determined by a fluorescein isothiocyanate (FITC)-labeled (green) 70-kDa dextran (**F**). Leakage of dextran into tissue surrounding the vasa vasorum could be detected (**F**, *). Dotted lines indicate the outline of the carotid artery, which is situated below the vasa vasorum. Bars indicate 100 μm (**A** and **B**) or 25 μm (**C**–**F**).

exclusively located at atherosclerotic foci around the carotid bifurcation and were neither observed further upstream at the nondiseased common carotid artery nor in younger ApoE$^{-/-}$ mice or age-matched C57Bl/6 controls (Table 2). Individual endothelial cells (Figure 1C, arrowheads) of the vasa vasorum and their nuclei (Figure 1C, arrows) could be delineated.

In vivo measurements displayed a predominantly arterial phenotype of the vasa vasorum (Figure 1D), as observed by Ephrin-B2 and Eph-B4 staining. Moreover, on local or bilateral ligation of the jugular vein for up to 30 minutes, functional parameters (eg, microvessel diameter) remained unaltered (Figure II in the online-only Data Supplement), arguing a marginal role of the venous system in controlling the vasa vasorum.

Plaque-Associated Vasa Vasorum Showed Angiogenic Activity In Vivo

The particular localization of the microvasculature at sites of plaque formation and absence of microvasculature in young atherosclerotic mice suggests angiogenesis underlies the development of these microvessels. Therefore, a cyclic Asn–Gly–Arg probe targeting the angiogenic marker CD13 and specific for angiogenic endothelium on in vivo injection[26] was used to investigate whether ongoing angiogenesis was present. The vasa vasorum showed CD31^{+}/CD13^{-} microvessels accompanied by occasional CD31^{low}/CD13^{+} sprouts (Figure 1E). At the site of sprouting, part of the endothelium expressed both CD31 and CD13 (Figure 1E, inset).

Table 2. Prevalence of Adventitial Vasa Vasorum in the Carotid Artery in the Various Experimental Groups

		Adventitial Microvessels		
Genotype	No. of Mice	No	Yes	% Present
C57Bl/6	20	20	0	0*
ApoE$^{-/-}$ (<16 wk)	8	7	1	12.5*
ApoE$^{-/-}$ (>40 wk)	51	6	45	88.2*

ApoE$^{-/-}$ indicates apolipoprotein E–deficient.
*P<0.0001; Fisher exact test; vs aged ApoE$^{-/-}$.

Plaque-Associated Vasa Vasorum Were Actively Perfused and Hyperpermeable

Because the normal physiology and perfusion of vasa vasorum microvessels were unknown, this was assessed by injection of 70-kDa and 150-kDa fluorescein isothiocyanate-dextrans, which indicated active perfusion (Figure 1F, green) of the vasa vasorum (red: CD31) in vivo. Also, sprouting of new microvessels was observed (Figure 1F, arrowhead), with new sprouts displaying low CD31 expression. Additionally, a rise in fluorescence intensity (ie, dextran concentration) in the adventitia was observed (Figure 1F, asterisk).

Concurrently, dextran injection allowed measurement of microvascular permeability by calculating the time-dependent rise in extraluminal fluorescence intensity compared with intraluminal fluorescence intensity. Although intraluminal dextran levels remained constant for >60 minutes, the extraluminal content of 70-kDa dextran increased with time to an extraluminal/intraluminal ratio of ≈0.46 after 35 minutes in

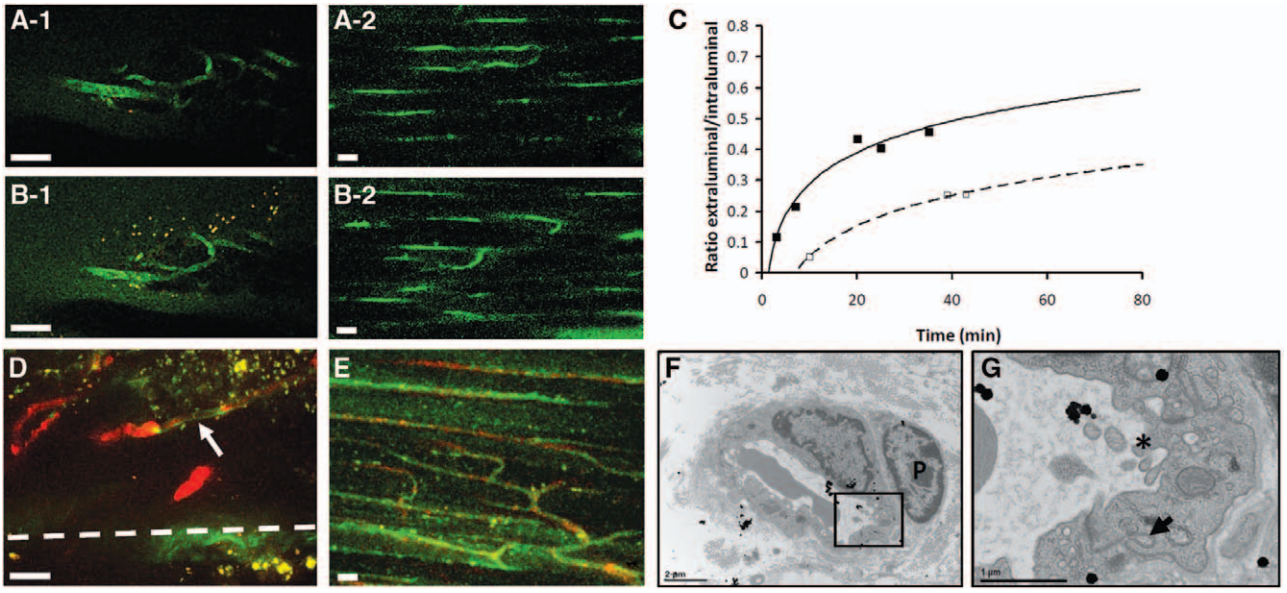

Figure 2. Microvascular permeability was calculated from the ratio of the extraluminal/intraluminal fluorescence intensity of 70-kDa fluorescein isothiocyanate (FITC)-dextran. Extraluminal fluorescence intensity increased over time, as depicted for t=3 and t=35 minutes after injection (**A-1** and **B-1**, respectively) for vasa vasorum, whereas only a limited increase in fluorescence intensity was observed for the control sternohyoid muscle at the same time points (**A-2** and **B-2**, respectively). The ratio extraluminal/intraluminal fluorescence intensity was calculated for different time points, as shown in a representative plot (**C**). Over time, the extraluminal presence of 70-kDa FITC-dextran increased significantly in the vasa vasorum (black line), but not in control microvessels (dotted line). No significant microvascular leakage was observed for 150-kDa dextrans in either vessel types (not shown). In plaque-associated vasa vasorum (**D**), the glycocalyx (green: wheat germ agglutinin [WGA]) was present in only a small part of the microvessel (**arrow**; red: CD31). In contrast, the glycocalyx was consistently present in control microvessels in the sternohyoid muscle (**E**). Interendothelial junctions in plaque-associated vasa vasorum were, however, intact (**F**, higher magnification in **G**; **arrows**), although the endothelial cells did show signs of membrane blebbing (*). Pericytes (P) surrounding the endothelial cells were also found. Dotted line indicates the outline of the carotid artery, which is situated below the vasa vasorum; bars indicate 25 μm (**A**–**E**).

plaque-associated vasa vasorum (Figure 2A-1 and 2B-1). Because vasa vasorum, in accordance with literature,[19,31] was not observed in nondiseased arteries, we used the similar sized microvasculature of the nearby sternohyoid muscle as a control. In the sternohyoid muscle, only a limited increase in extravascular dextran concentration was observed (Figure 2A-2 and 2B-2). On quantification, extravascular dextran concentration (Figure 2C, black line, $P<0.05$) was significantly increased only in vasa vasorum, but not in control microvessels (Figure 2C, dotted line), indicative of enhanced microvascular permeability in the vasa vasorum. Additionally, extravasation of 70-kDa dextran occurred earlier in vasa vasorum compared with control microvessels (Figure 2C). Because of myocyte autofluorescence, baseline extra/intraluminal fluorescence ratios varied slightly; however, all experiments showed an identical pattern of significantly increased microvascular permeability of the vasa vasorum. Of note, microvascular extravasation of 150-kDa dextran did not significantly increase over time, neither in the vasa vasorum or in control microvessels (not shown).

A size-dependent increase in permeability could be caused by several mechanisms. It is known that reduction or absence of endothelial glycocalyx in microvessels can, independently from the interendothelial junctions, lead to increased permeability and leukocyte adhesion.[32] In addition, disruption of the endothelial barrier may cause hyperpermeability. To determine what caused the increased permeability, we examined glycocalyx integrity by wheat germ agglutinin staining and analyzed the integrity of the interendothelial junctions by electron microscopy. Staining for wheat germ agglutinin in vivo showed an irregular staining pattern in the vasa vasorum (Figure 2D), contrary to an evenly distributed expression of glycocalyx throughout control microvessels in the sternohyoid muscle (Figure 2E; Figure III in the online-only Data Supplement). The interendothelial junctions were intact as shown by electron microscopy (Figure 2F and 2G; arrows), and occasionally, pericytes (P) were found covering the microvascular endothelium. The endothelial cells did, however, show initial signs of membrane blebbing, indicative of early endothelial dysfunction.

Plaque-Associated Vasa Vasorum Showed Decreased Blood Flow, Yet an Increased Adhesion and Extravasation of Leukocytes

Leukocytes were observed within the vasa vasorum after in vitro (Figure 3A) and in vivo (Figure 3B, Figure II in the online-only Data Supplement) labeling. Using labeled leukocytes and platelets, blood flow velocity and blood flow were assessed in the carotid artery, vasa vasorum, and control microvessels. Both blood flow velocity (2.1-fold decrease, $P<0.001$; Figure 3C, Table I in the online-only Data Supplement) and blood flow (7.6–9.8-fold decrease, $P<0.001$; Figure 3D) were significantly reduced in vasa vasorum compared with control microvessels. Changes in blood flow and flow velocity were independent of microvessel diameter. Blood flow direction was identical to the main artery.

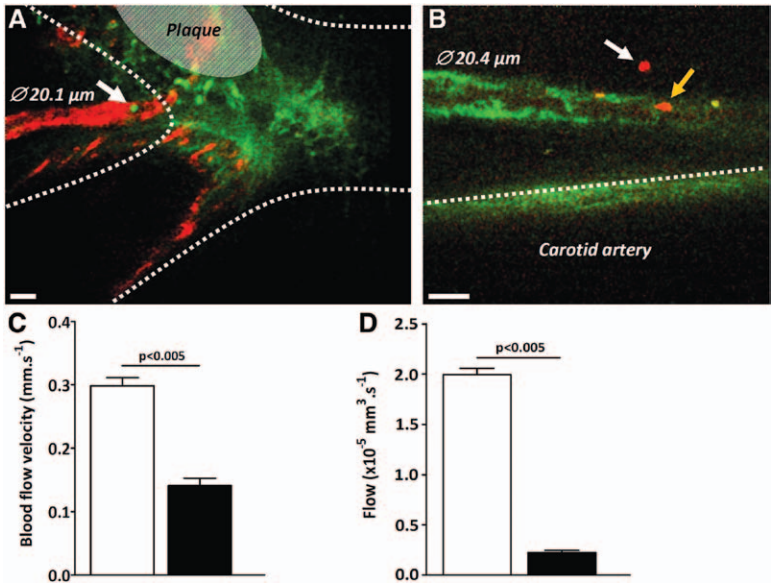

Figure 3. Cellular perfusion (**A**; green, **arrow**) of vasa vasorum (**A**; red) in aged apolipoprotein E–deficient (ApoE$^{-/-}$) mice. **A**, Vascular endothelium (red) and elastin autofluorescence (green) of the carotid artery are also visible. Leukocytes (**B**; red) adhered to (**yellow arrow**) or extravasated from (**white arrow**) the vasa vasorum (**B**; green). Dotted lines indicate the outline of the carotid artery, situated below the vasa vasorum; bars indicate 25 µm. Leukocyte velocity in vasa vasorum (black bars, **C**) is significantly reduced compared with control microvessels (white bars, **C**). Blood flow in vasa vasorum is also significantly lower than in control microvessels (**D**). Dotted line indicates the outline of the carotid artery; bars indicate 25 µm.

Additionally, adhesion and transmigration of ex vivo and in vivo labeled leukocytes were significantly increased compared with control microvessels (Figure 4). Increased adhesion (Figure 4A, $1.3\times10^{-2}\pm0.3\times10^{-2}$ versus $0.2\times10^{-2}\pm0.1\times10^{-2}$ cells/mm^2 per minute, $P<0.05$) and extravasation (Figure 4B, $1.8\times10^{-2}\pm0.4\times10^{-2}$ versus $0.3\times10^{-2}\pm0.2\times10^{-2}$ cells/mm^2 per minute, $P<0.05$) of leukocytes were observed in plaque-associated vasa vasorum and control microvessels, respectively. Leukocyte adhesion and extravasation were examined in more detail ex vivo, using 3-dimensional image analysis. Cell morphology suggested transmigration of different leukocyte subtypes, including pseudopodia-rich cells resembling a dendritic morphology, from the vasa vasorum toward the plaque (Figure 4C and 4D, Movie III in the online-only Data Supplement).

Ex Vivo MPLSM Confirmed Presence of Vasa Vasorum and Intraplaque Microvascular Structures

Plaque-associated vasa vasorum were also imaged ex vivo, allowing imaging at higher resolution and signal-to-noise

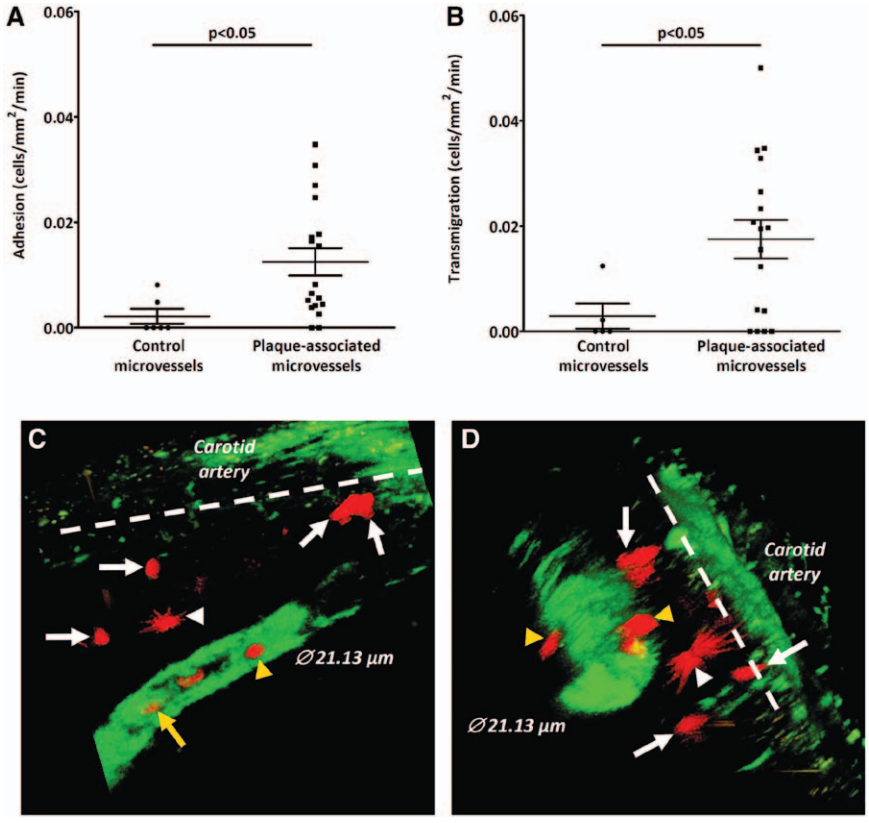

Figure 4. In aged apolipoprotein E–deficient (ApoE$^{-/-}$) mice, adhesion and extravasation were significantly increased in vasa vasorum compared with control microvessels of similar diameters (**A** and **B**). This is accompanied by decreased blood flow (see Figure 3**C** and 3**D**). Three-dimensional reconstruction (**C** and **D**) of in situ z-scan showed adhering (**yellow arrow**) and transmigrated cells (**white arrows**), as well as cells in the progress of transmigration through the microvessel wall (**yellow arrowheads**). Multiphoton laser scanning microscopy (MPLSM) allowed differentiation of morphologically distinct cell types (eg, pseudopodia-rich cells resembling a dendritic morphology; **white arrowheads**).

ratio without motion artifacts. For ex vivo imaging, the carotid artery or abdominal aorta was excised, mounted in a perfusion chamber and imaged under a transmural pressure of 80 mm Hg to mimic physiological conditions.[24] Ex vivo imaging was performed up to 30 μm from the outer elastic lamina. Vasa vasorum were detected both in the carotid artery and abdominal aorta (Table 1).

Ex vivo imaging clearly visualized intraplaque microvascular structures (Figure IVA and IVB in the online-only Data Supplement), yet intraplaque microvessels were only found in 6 of 20 plaques (Table II in the online-only Data Supplement). Surprisingly, none of these microvessels derived from the vasa vasorum. Rather, data suggested that these microvessels originated from endothelial sprouting from the luminal endothelial layer (3 of 6 plaques; Figure IVC in the online-only Data Supplement). No functional characteristics could be determined for intraplaque vessels, arguing a limited role for intraplaque microvessels in this model. Also, occurrence of intraplaque hemorrhage (IPH) was determined in aged ApoE$^{-/-}$, and was found in 4 of 20 (20%) mice examined. Although all mice that showed IPH also showed vasa vasorum, only a minor fraction of vasa vasorum–containing plaques showed features of IPH. Occurrence of IPH could not be linked to occurrence of luminal microvascular structures.

Discussion

The presence and role of plaque-associated microvessels in murine plaques have been extensively debated in literature. Previous attempts to detect these microvessels yielded varying results, in part depending on the animal model and visualization techniques used. Here, we used in vivo MPLSM to show that plaque-associated vasa vasorum (1) are present in ApoE$^{-/-}$ mice; (2) show angiogenic activity; (3) are actively perfused and hyperpermeable; (4) have significantly reduced blood flow and blood flow velocity compared with control microvessels with similar diameter, and (5) show enhanced leukocyte adhesion and transmigration at the site of the atherosclerotic plaque. Taken together, we show that plaque-associated microvessels exhibit functional features that could facilitate plaque development and progression.

The increased adhesion of leukocytes may, in part, be a consequence of the reduction in blood flow velocity, because this would cause a reduction in local shear stress at the microvascular wall. Consequently, low shear stress is deemed to cause endothelial cell dysfunction and upregulation of adhesion molecules like vascular cell adhesion molecule-1 and intercellular adhesion molecule-1.[33–35] The increased leukocyte adhesion was accompanied by augmented transmigration to the adventitial tissue, facilitating a second site of ingress of leukocytes, besides migration through the luminal endothelium. These cells may contribute to further plaque development, either by functioning in the adventitia itself, or by infiltration into the plaque after migrating through the media. As such, the vasa vasorum could contribute to exacerbation of atherosclerosis, by infiltration of new inflammatory cells.[36]

Additionally, vasa vasorum hyperpermeability may be another important contributor to plaque progression, as it favors extravasation of lipids and plasma proteins at sites of plaque development.[37] Increased permeability may be attributed to disruption of the endothelial barrier function.[10] Our finding of augmented microvascular extravasation in the vasa vasorum, at least for molecules with a molecular weight of up to 70 kDa, suggests that abundant plasma proteins, such as albumin, can leak into the adventitia. Indeed, extravascular albumin has been detected in both human and mouse atherosclerotic lesions.[38,39] Here, we extend these findings, demonstrating an apparent size limit for endothelial leakage in vasa vasorum of 70 to 150 kDa in vivo in aged ApoE$^{-/-}$ mice. The origin of the microvascular hyperpermeability remains to be further elucidated. Electron microscopy did not show any aberrations in endothelial cell junctions, concordant with a recent study from Eriksson.[31] However, the endothelial glycocalyx of plaque-associated vasa vasorum was disrupted, indicating a possible cause for the increase in vascular permeability, and more specifically, permeability for smaller molecules. Both the increased leukocyte extravasation and hyperpermeability will affect plaque development and progression, especially when plaques become more advanced and vasa vasorum has expanded by increasing adventitial inflammation. As such, these processes could enhance plaque progression independent of microvascular disruption and hemorrhage.

Vasa vasorum were abundantly present at sites of atherosclerotic plaques, sites at which we also observed an increase in vessel wall thickness (not shown). Thickening of the vessel wall may infer an increase in vascularization, because oxygenation of the entire tissue is hindered by vessel wall thickening, potentially increasing local hypoxia. Remarkably, although the entire carotid artery was examined, we did not observe any vascularization of nonatherosclerotic segments, neither in control animals nor in the young or aged ApoE$^{-/-}$ mice. This is consistent with reports by, for example, Gräbner et al[40] or Eriksson.[31] Given the fact that vasa vasorum were absent in nonatherosclerotic segments, we chose the sternohyoid microvasculature as a substitute model for general microvascular blood flow. Taken together, development of vasa vasorum in ApoE$^{-/-}$ mice appears to be an adaptive response to pathological, atherosclerosis-induced vessel wall changes.

Many studies have suggested a role for angiogenesis in atherosclerosis. Proatherogenic effects of increased angiogenesis and antiatherogenic effects on decreased angiogenesis have been described in models of pharmacological stimulation or inhibition of angiogenesis,[18,19,41] as well as in certain animal models (eg, the collagen-XVIII/ApoE double knockout mouse).[15] Here, presence of CD13^{+}/CD31^{low} sprouts in the adventitia substantiates the presence of ongoing angiogenesis. The reduced expression of CD31 is in accordance with studies that have shown that both embryonic stem cells and mature endothelial cells show reduced expression of CD31 during endothelial differentiation, migration, and proliferation.[42,43] It is, however, surprising that the plaque-associated vasa vasorum showed an almost exclusively arterial phenotype, which is in contrast to the model suggested by Eriksson.[31] Possibly, this is attributable to differences in experimental setup, as the current study was performed on mice without a diet and at a younger age than the mice used by Eriksson, resulting in a less developed vasa vasorum. On the other hand, it should be noted that Ephrin-B2 is known to be expressed on angiogenic endothelium and, therefore, could account for the increased

Ephrin-B2 staining. However, because there was no response to venous ligation, it is conceivable that the vasa vasorum in fact may drain on the carotid artery, acting comparable with an arterial shunt. This would explain the low flow, which could be a consequence of a small pressure gradient over the vasa vasorum, although the latter may also be influenced by pulsation caused by systolic and diastolic phases of the cardiac cycle.

Whereas plaque-associated microvessels were primarily located in the adventitia surrounding the atherosclerotic lesion, vessel-like structures were sporadically detected within the plaque itself (Table II in the online-only Data Supplement). Surprisingly, these structures did not originate from the vasa vasorum, because microvessels did not traverse the media. These findings oppose observations in human plaques.[8] Of note, incidental sprouting from the luminal endothelium was observed, yet these intraplaque vascular structures did not seem to be functionally perfused in vivo. Lucerna et al[13] showed that overexpression of vascular endothelial growth factor in mice led to more luminal invaginations, accompanied by an increased leukocyte influx into the plaque. Therefore, intraplaque microvascular structures, even when originating from the lumen, may contribute to the progression of atherosclerotic plaques in mice. Additionally, intimal microvessels are suggested to be causal for IPH, although no causal link between IPH and plaque vascularization could be discerned. The observed occurrence of IPH was within the range described in, for example, the studies from Rosenfeld,[44] Calara,[45] and Johnson,[46] which however show a large variation in the occurrence of IPH (3.6%–75%). Generally, proof of a causal relationship between vascularization and IPH is lacking in murine models, which is substantiated by our current study. The data, however, are suggestive of a contribution of vasa vasorum to IPH, or plaque instability in general, although the presence of vasa vasorum does not infer occurrence of IPH.

Although this murine model does not completely mimic human atherosclerosis, because it only shows a limited, yet consistent occurrence of (intraplaque) vascularization, it provides new insights into the potential role of vasa vasorum in human atherosclerosis. Importantly, a number of features found in our study are consistent with previous studies in human atherosclerosis. For example, human plaque microvessels have been associated with ingress of leukocytes and erythrocytes and with leakage of albumin.[2] In this study, we established increased leukocyte adhesion and extravasation from adventitial microvessels, as well as an increased permeability of microvessels for 70-kDa dextrans, resembling albumin leakage in human atherosclerosis. Interestingly, and in contrast to our model, human plaque microvessels generally seem to have a more instable microvascular phenotype and show disrupted interendothelial junctions,[10] especially in intraplaque microvessels. Hence, it would be interesting to investigate functional features of plaque neovascularization in other murine models, which have already described intraplaque microvessels or more extensive vasa vasorum expansion.[15,47]

In summary, using a novel in vivo imaging strategy, we were able to study plaque-associated microvessels in mice and quantify its functional characteristics. The plaque-associated vasa vasorum demonstrated a significantly reduced blood flow, blood flow velocity, as well as an increase in leukocyte adhesion, leukocyte transmigration, and endothelial permeability compared with control microvasculature. In conjunction with the ongoing angiogenic activity, these features would support progression of atherosclerotic lesions. Further studies will help unravel by which means microvascular function in the vasa vasorum may be normalized.

Sources of Funding

This project was funded by institutional funding and the Established Investigator grant 2003T2001 (E.A.L. Biessen) of the Netherlands Heart Foundation.

Disclosures

None.

References

1. Sluimer JC, Daemen MJ. Novel concepts in atherogenesis: angiogenesis and hypoxia in atherosclerosis. *J Pathol*. 2009;218:7–29.
2. Virmani R, Kolodgie FD, Burke AP, Finn AV, Gold HK, Tulenko TN, Wrenn SP, Narula J. Atherosclerotic plaque progression and vulnerability to rupture: angiogenesis as a source of intraplaque hemorrhage. *Arterioscler Thromb Vasc Biol*. 2005;25:2054–2061.
3. Köster W. Endarteritis and arteritis. *Berl Klin Wochenschr*. 1876;13:343–345
4. Gössl M, Versari D, Mannheim D, Ritman EL, Lerman LO, Lerman A. Increased spatial vasa vasorum density in the proximal LAD in hypercholesterolemia–implications for vulnerable plaque-development. *Atherosclerosis*. 2007;192:246–252.
5. Moreno PR, Purushothaman KR, Fuster V, Echeverri D, Truszczynska H, Sharma SK, Badimon JJ, O'Connor WN. Plaque neovascularization is increased in ruptured atherosclerotic lesions of human aorta: implications for plaque vulnerability. *Circulation*. 2004;110:2032–2038.
6. de Boer OJ, van der Wal AC, Teeling P, Becker AE. Leucocyte recruitment in rupture prone regions of lipid-rich plaques: a prominent role for neovascularization? *Cardiovasc Res*. 1999;41:443–449.
7. Jeziorska M, Woolley DE. Local neovascularization and cellular composition within vulnerable regions of atherosclerotic plaques of human carotid arteries. *J Pathol*. 1999;188:189–196.
8. Kumamoto M, Nakashima Y, Sueishi K. Intimal neovascularization in human coronary atherosclerosis: its origin and pathophysiological significance. *Hum Pathol*. 1995;26:450–456.
9. Sluimer JC, Gasc JM, van Wanroij JL, Kisters N, Groeneweg M, Sollewijn Gelpke MD, Cleutjens JP, van den Akker LH, Corvol P, Wouters BG, Daemen MJ, Bijnens AP. Hypoxia, hypoxia-inducible transcription factor, and macrophages in human atherosclerotic plaques are correlated with intraplaque angiogenesis. *J Am Coll Cardiol*. 2008;51:1258–1265.
10. Sluimer JC, Kolodgie FD, Bijnens AP, Maxfield K, Pacheco E, Kutys B, Duimel H, Frederik PM, van Hinsbergh VW, Virmani R, Daemen MJ. Thin-walled microvessels in human coronary atherosclerotic plaques show incomplete endothelial junctions relevance of compromised structural integrity for intraplaque microvascular leakage. *J Am Coll Cardiol*. 2009;53:1517–1527.
11. Moos MP, John N, Gräbner R, Nossmann S, Günther B, Vollandt R, Funk CD, Kaiser B, Habenicht AJ. The lamina adventitia is the major site of immune cell accumulation in standard chow-fed apolipoprotein E-deficient mice. *Arterioscler Thromb Vasc Biol*. 2005;25:2386–2391.
12. Celletti FL, Waugh JM, Amabile PG, Brendolan A, Hilfiker PR, Dake MD. Vascular endothelial growth factor enhances atherosclerotic plaque progression. *Nat Med*. 2001;7:425–429.
13. Lucerna M, Zernecke A, de Nooijer R, de Jager SC, Bot I, van der Lans C, Kholova I, Liehn EA, van Berkel TJ, Yla-Herttuala S, Weber C, Biessen EA. Vascular endothelial growth factor-A induces plaque expansion in ApoE knock-out mice by promoting de novo leukocyte recruitment. *Blood*. 2007;109:122–129.
14. Luttun A, Tjwa M, Carmeliet P. Placental growth factor (PlGF) and its receptor Flt-1 (VEGFR-1): novel therapeutic targets for angiogenic disorders. *Ann N Y Acad Sci*. 2002;979:80–93.
15. Moulton KS, Olsen BR, Sonn S, Fukai N, Zurakowski D, Zeng X. Loss of collagen XVIII enhances neovascularization and vascular permeability in atherosclerosis. *Circulation*. 2004;110:1330–1336.

16. Tanaka K, Nagata D, Hirata Y, Tabata Y, Nagai R, Sata M. Augmented angiogenesis in adventitia promotes growth of atherosclerotic plaque in apolipoprotein E-deficient mice. *Atherosclerosis*. 2011;215:366–373.
17. Hauer AD, van Puijvelde GH, Peterse N, de Vos P, van Weel V, van Wanrooij EJ, Biessen EA, Quax PH, Niethammer AG, Reisfeld RA, van Berkel TJ, Kuiper J. Vaccination against VEGFR2 attenuates initiation and progression of atherosclerosis. *Arterioscler Thromb Vasc Biol*. 2007;27:2050–2057.
18. Moulton KS, Heller E, Konerding MA, Flynn E, Palinski W, Folkman J. Angiogenesis inhibitors endostatin or TNP-470 reduce intimal neovascularization and plaque growth in apolipoprotein E-deficient mice. *Circulation*. 1999;99:1726–1732.
19. Moulton KS, Vakili K, Zurakowski D, Soliman M, Butterfield C, Sylvin E, Lo KM, Gillies S, Javaherian K, Folkman J. Inhibition of plaque neovascularization reduces macrophage accumulation and progression of advanced atherosclerosis. *Proc Natl Acad Sci USA*. 2003;100:4736–4741.
20. Petrovan RJ, Kaplan CD, Reisfeld RA, Curtiss LK. DNA vaccination against VEGF receptor 2 reduces atherosclerosis in LDL receptor-deficient mice. *Arterioscler Thromb Vasc Biol*. 2007;27:1095–1100.
21. Calcagno C, Cornily JC, Hyafil F, Rudd JH, Briley-Saebo KC, Mani V, Goldschlager G, Machac J, Fuster V, Fayad ZA. Detection of neovessels in atherosclerotic plaques of rabbits using dynamic contrast enhanced MRI and 18F-FDG PET. *Arterioscler Thromb Vasc Biol*. 2008;28:1311–1317.
22. Winter PM, Morawski AM, Caruthers SD, Fuhrhop RW, Zhang H, Williams TA, Allen JS, Lacy EK, Robertson JD, Lanza GM, Wickline SA. Molecular imaging of angiogenesis in early-stage atherosclerosis with alpha(v)beta3-integrin-targeted nanoparticles. *Circulation*. 2003;108:2270–2274.
23. Langheinrich AC, Michniewicz A, Sedding DG, Walker G, Beighley PE, Rau WS, Bohle RM, Ritman EL. Correlation of vasa vasorum neovascularization and plaque progression in aortas of apolipoprotein E(-/-)/low-density lipoprotein(-/-) double knockout mice. *Arterioscler Thromb Vasc Biol*. 2006;26:347–352.
24. Megens RT, Reitsma S, Schiffers PH, Hilgers RH, De Mey JG, Slaaf DW, oude Egbrink MG, van Zandvoort MA. Two-photon microscopy of vital murine elastic and muscular arteries. Combined structural and functional imaging with subcellular resolution. *J Vasc Res*. 2007;44:87–98.
25. van Zandvoort M, Engels W, Douma K, Beckers L, Oude Egbrink M, Daemen M, Slaaf DW. Two-photon microscopy for imaging of the (atherosclerotic) vascular wall: a proof of concept study. *J Vasc Res*. 2004;41:54–63.
26. Buehler A, van Zandvoort MA, Stelt BJ, Hackeng TM, Schrans-Stassen BH, Bennaghmouch A, Hofstra L, Cleutjens JP, Duijvestijn A, Smeets MB, de Kleijn DP, Post MJ, de Muinck ED. cNGR: a novel homing sequence for CD13/APN targeted molecular imaging of murine cardiac angiogenesis in vivo. *Arterioscler Thromb Vasc Biol*. 2006;26:2681–2687.
27. Oostendorp M, Douma K, Wagenaar A, Slenter JM, Hackeng TM, van Zandvoort MA, Post MJ, Backes WH. Molecular magnetic resonance imaging of myocardial angiogenesis after acute myocardial infarction. *Circulation*. 2010;121:775–783.
28. Megens RT, Reitsma S, Prinzen L, oude Egbrink MG, Engels W, Leenders PJ, Brunenberg EJ, Reesink KD, Janssen BJ, ter Haar Romeny BM, Slaaf DW, van Zandvoort MA. *In vivo* high-resolution structural imaging of large arteries in small rodents using two-photon laser scanning microscopy. *J Biomed Opt*. 2010;15:011108.
29. Yu W, Braz JC, Dutton AM, Prusakov P, Rekhter M. *In vivo* imaging of atherosclerotic plaques in apolipoprotein E deficient mice using nonlinear microscopy. *J Biomed Opt*. 2007;12:054008.
30. Kamoun WS, Chae SS, Lacorre DA, Tyrrell JA, Mitre M, Gillissen MA, Fukumura D, Jain RK, Munn LL. Simultaneous measurement of RBC velocity, flux, hematocrit and shear rate in vascular networks. *Nat Methods*. 2010;7:655–660.
31. Eriksson EE. Intravital microscopy on atherosclerosis in apolipoprotein e-deficient mice establishes microvessels as major entry pathways for leukocytes to advanced lesions. *Circulation*. 2011;124:2129–2138.
32. van den Berg BM, Vink H, Spaan JA. The endothelial glycocalyx protects against myocardial edema. *Circ Res*. 2003;92:592–594.
33. Alon R, Ley K. Cells on the run: shear-regulated integrin activation in leukocyte rolling and arrest on endothelial cells. *Curr Opin Cell Biol*. 2008;20:525–532.
34. Dekker RJ, van Thienen JV, Rohlena J, de Jager SC, Elderkamp YW, Seppen J, de Vries CJ, Biessen EA, van Berkel TJ, Pannekoek H, Horrevoets AJ. Endothelial KLF2 links local arterial shear stress levels to the expression of vascular tone-regulating genes. *Am J Pathol*. 2005;167:609–618.
35. Mestas J, Ley K. Monocyte-endothelial cell interactions in the development of atherosclerosis. *Trends Cardiovasc Med*. 2008;18:228–232.
36. Jeziorska M, Woolley DE. Neovascularization in early atherosclerotic lesions of human carotid arteries: its potential contribution to plaque development. *Hum Pathol*. 1999;30:919–925.
37. Doyle B, Caplice N. Plaque neovascularization and antiangiogenic therapy for atherosclerosis. *J Am Coll Cardiol*. 2007;49:2073–2080.
38. Lobbes MB, Miserus RJ, Heeneman S, Passos VL, Mutsaers PH, Debernardi N, Misselwitz B, Post M, Daemen MJ, van Engelshoven JM, Leiner T, Kooi ME. Atherosclerosis: contrast-enhanced MR imaging of vessel wall in rabbit model–comparison of gadofosveset and gadopentetate dimeglumine. *Radiology*. 2009;250:682–691.
39. Zhang Y, Cliff WJ, Schoefl GI, Higgins G. Immunohistochemical study of intimal microvessels in coronary atherosclerosis. *Am J Pathol*. 1993;143:164–172.
40. Gräbner R, Lötzer K, Döpping S, et al. Lymphotoxin beta receptor signaling promotes tertiary lymphoid organogenesis in the aorta adventitia of aged ApoE-/- mice. *J Exp Med*. 2009;206:233–248.
41. Bot I, Jukema JW, Lankhuizen IM, van Berkel TJ, Biessen EA. Atorvastatin inhibits plaque development and adventitial neovascularization in ApoE deficient mice independent of plasma cholesterol levels. *Atherosclerosis*. 2011;214:295–300.
42. Li ZJ, Wang ZZ, Zheng YZ, Xu B, Yang RC, Scadden DT, Han ZC. Kinetic expression of platelet endothelial cell adhesion molecule-1 (PECAM-1/CD31) during embryonic stem cell differentiation. *J Cell Biochem*. 2005;95:559–570.
43. RayChaudhury A, Elkins M, Kozien D, Nakada MT. Regulation of PECAM-1 in endothelial cells during cell growth and migration. *Exp Biol Med (Maywood)*. 2001;226:686–691.
44. Rosenfeld ME, Polinsky P, Virmani R, Kauser K, Rubanyi G, Schwartz SM. Advanced atherosclerotic lesions in the innominate artery of the ApoE knockout mouse. *Arterioscler Thromb Vasc Biol*. 2000;20:2587–2592.
45. Calara F, Silvestre M, Casanada F, Yuan N, Napoli C, Palinski W. Spontaneous plaque rupture and secondary thrombosis in apolipoprotein E-deficient and LDL receptor-deficient mice. *J Pathol*. 2001;195:257–263.
46. Johnson JL, Jackson CL. Atherosclerotic plaque rupture in the apolipoprotein E knockout mouse. *Atherosclerosis*. 2001;154:399–406.
47. Khatri JJ, Johnson C, Magid R, Lessner SM, Laude KM, Dikalov SI, Harrison DG, Sung HJ, Rong Y, Galis ZS. Vascular oxidant stress enhances progression and angiogenesis of experimental atheroma. *Circulation*. 2004;109:520–525.